Ring of C_{60} Polymers Formed by Electron or Hole Injection from a Scanning Tunneling Microscope Tip

Ryo Nouchi,[1,2,*] Kosuke Masunari,[2] Toshio Ohta,[2] Yoshihiro Kubozono,[1,2,†] and Yoshihiro Iwasa[1,3]

[1]*CREST, Japan Science and Technology Agency, Kawaguchi 322-0012, Japan*
[2]*Department of Chemistry, Okayama University, Okayama 700-8530, Japan*
[3]*Institute for Materials Research, Tohoku University, Sendai 980-8577, Japan*

(Received 14 February 2006; revised manuscript received 31 May 2006; published 7 November 2006)

Carrier (electron or hole) injection from a scanning tunneling microscope tip causes various surface modifications on the molecular scale. We report that injection into C_{60} close-packed layers forms a ring-shaped distribution of C_{60} polymers. This can be explained on the basis of the radial propagation and energy dissipation of carriers. Subsequent electron or hole injections enlarge the ring, showing that both carriers can induce both polymerization and depolymerization. Furthermore, we demonstrate visualization of carrier scattering by injecting carriers into C_{60} layers with grain boundaries.

DOI: 10.1103/PhysRevLett.97.196101 PACS numbers: 68.37.Ef, 61.48.+c, 73.50.−h, 82.35.−x

Scanning tunneling microscopy (STM) is a powerful technique for the atomic and molecular scale imaging and modification of various surfaces. Carrier (electron or hole) injection from a STM tip causes the movement and extraction of surface atoms [1,2] (molecules [3,4]), and various types of chemical reactions [5–8]. In the case of carrier injection into close-packed layers of C_{60}, polymerization of C_{60} molecules has been reported by several groups [5,7,8], and we recently performed nanoscale patterning by manipulation (removal and movement) of single C_{60} molecules [4]. In this Letter we observed a formation of ring-shaped distributions of C_{60} polymers and established a technique to control the radius of the ring by sequential electron or hole injections. The result is reasonably explained by taking into account the difference in energies necessary for polymerization and depolymerization. Furthermore, a visualization of carrier scattering is achieved by imaging the shapes of resultant rings formed by carrier injection into C_{60} close-packed layers with crystalline defects that act as carrier scatterers.

A close-packed structure of C_{60} was formed on a Si(111) − 7 × 7 surface as described elsewhere [4]. C_{60} molecules adsorbed on a bare Si surface are immobile because of the strong interactions with Si dangling bonds, so that the first monolayer did not show a long-range ordering. An ordered close-packed structure was, therefore, formed in the multilayer of C_{60}. In order to induce polymerization of C_{60} molecules, carrier injection from a STM tip was performed by application of voltage pulses with durations of 30 s. During carrier injection, a constant-current feedback control loop was turned off in order to maintain the tip-sample separation at a distance defined by a sample bias voltage, V_S, of 2.0 V and a tunneling current, I_t, of 0.2 nA. STM images were obtained under the feedback control with V_S of 2.0 V and I_t of 0.2 nA. All experiments were performed with a W tip at room temperature.

Figure 1(a) shows a STM image of a C_{60} close-packed multilayer obtained after carrier injection at +3.3 V into the marked point. A beautiful ring-shaped distribution of dim spots was formed by the injection, although an incomplete ring of C_{60} polymers was previously reported [7]. For identification of structures of the ring patterns, we have taken a high-resolution image of the portion of a ring [Fig. 1(b)]. Since C_{60} molecules in a close-packed layer exhibit free rotation at room temperature [9], their internal electronic structures are not observed in STM images at room temperature. In sharp contrast, the internal structures

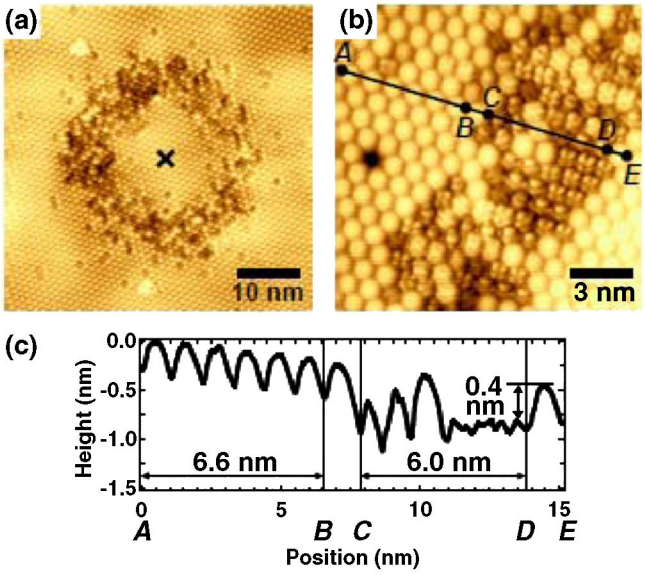

FIG. 1 (color online). (a) STM image of a C_{60} close-packed multilayer acquired after carrier injection into the marked point at +3.3 V. Bright and dim spots in the image represent C_{60} monomers and polymerized C_{60} molecules, respectively. (b) High-resolution image of a portion of a ring. (c) Height profile measured along the line from A to E in (b). A dent of 0.4 nm is observed at a polymerized molecule located at the left of D. Total sizes of six monomers and six dim molecules showing their internal electronic structures are 6.6 and 6.0 nm, respectively.

of the molecules forming the ring were clearly observed in the image shown in Fig. 1(b), indicating that the rotation of C_{60} molecules is suppressed on the dim spots. Figure 1(c) shows a height profile of the surface measured along the line from *A* to *E* in Fig. 1(b). The height difference between bright and dim regions was determined as 0.4 nm. This result strongly suggests the formation of intermolecular bonds along the vertical direction. Total sizes of bright six molecules from *A* to *B* and dim six molecules from *C* to *D* were determined to be 6.6 and 6.0 nm, respectively. This deduction should be accounted for by the formation of intermolecular bonding along the lateral directions. The absence of free rotation of C_{60} molecules and shrink of intermolecular distance provide firm evidence for the occurrence of polymerization of C_{60} molecules by carrier injection from the STM tip.

Figure 2 shows the evolution of a ring of C_{60} polymers by sequential injection of carriers from a STM tip into a close-packed multilayer of C_{60}. The injection point of carriers was fixed at the center of the ring, and only the height of the applied voltage pulse was varied. Figure 2(a) shows the STM image acquired after carrier injection at -3.0 V. Inner and outer diameters of the ring were 12 and 23 nm, respectively. The ring was enlarged by subsequent injection at -3.3 V to a ring with inner and outer diameters of 17 and 33 nm, respectively [Fig. 2(b)]. Further enlargement to a ring with dimensions of 26 and 38 nm was obtained by the pulse of $+3.0$ V [Fig. 2(d)]. Here, the injections with negative and positive bias polarities correspond to hole [Figs. 2(a) and 2(b)] and electron [Fig. 2(d)] injection, respectively. The enlargements of the outer diameter from 23 to 33 nm [from Fig. 2(a) to 2(b)] by hole injection and from 33 to 38 nm [from Fig. 2(b) to 2(d)] by electron injection indicate that both carrier injections can induce polymerization. In the same way, the enlargement of the inner diameter shows that both carrier injections can cause depolymerization.

It was reported previously that electron injection produced C_{60} polymers in a ringlike distribution, and two models were proposed for this phenomenon [7]: (i) The shortening of intermolecular distance accompanying polymerization should cause an internal stress which may assist depolymerization especially inside the polymerized area. (ii) An electric polarization force attracts the film surface toward the tip, causing an increase in the intermolecular distance beneath the tip and enhancing depolymerization. However, these models are not adequate to explain the experimental results shown in Figs. 2(b) and 2(c). The starting image [Fig. 2(b)] corresponds to a ring of C_{60} polymers formed by hole injection at -3.3 V. Further carrier injection at the same bias induces polymerization of C_{60} molecules inside the ring [Fig. 2(c)]. If the stress is responsible for depolymerization inside the ring, C_{60} polymers cannot be formed inside the ring because the stress field concentrates on the center. Furthermore, since the electric polarization force is unchanged for the carrier injection at the same bias voltage, the first ring shape [Fig. 2(b)] should be maintained in Fig. 2(c). Thus, the proposed models can be ruled out as explanations for the ring formation. One of the other possible models for the ring formation is thermal depolymerization [10] by Joule heat generated by a tunneling current. The Joule heat should be unchanged for the rings [Figs. 2(b) and 2(c)]. Since this leads to the same ring pattern, this model can also be ruled out.

We propose a possible model that spreading carriers themselves produce rings of C_{60} polymers. It is significant to note that any carrier injections do not break the ring structures. Injected carriers interact with inter- and/or intramolecular phonons through the electron-phonon coupling, and dissipate their energies gradually as they spread from the injected point [Fig. 3(a)]. If the energies necessary for polymerization, E_P, and depolymerization, E_d, are supplied by the spreading carriers, the ring formation requires $E_P < E_d$ as seen from Fig. 3(a) because the carriers with higher energies than E_P (E_d) can induce polymerization (depolymerization). Therefore, carrier injection at higher bias voltage results in a ring with a larger diameter. This model reasonably explains the bias dependence of the ring diameters shown in Figs. 2(a) and 2(b).

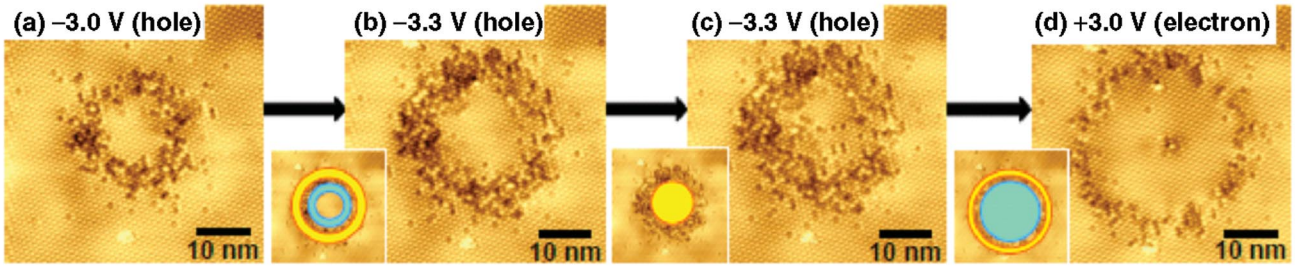

FIG. 2 (color). Evolution of a ring of C_{60} polymers by sequential carrier injection. STM images acquired sequentially after carrier injections into the same point with different V_S values. The injection point was at the center of the rings. Attached insets display areas in which polymerization (yellow) and depolymerization (blue) events occurred by the carrier injection. (a) Ring formed by hole injection at $V_S = -3.0$ V. (b) Ring enlarged by hole injection at -3.3 V. (c) Sequential hole injection at the same V_S induced polymerization around the center of the ring. (d) Ring enlarged by electron injection at $+3.0$ V.

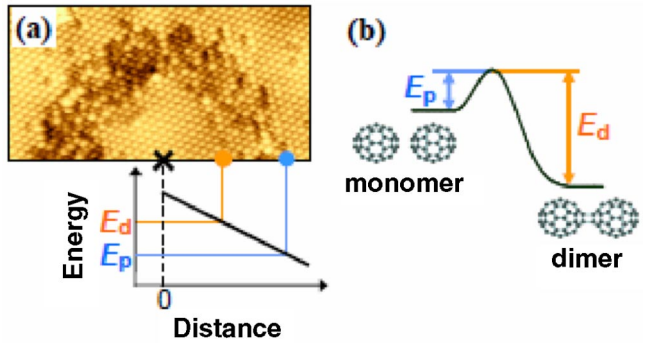

FIG. 3 (color online). Schematic picture of the model for the ring formation of C_{60} polymers. (a) Energy dissipation of injected carriers. The difference in energies necessary for polymerization, E_P, and depolymerization, E_d, forms the ring structure. (b) Potential curve for ionic polymerization and depolymerization reactions.

Note that the model is on the assumption of a simple band transport of charge carriers in a C_{60} crystal, where intermolecular van der Waals forces form narrow crystalline bands. This assumption is reasonable even for such narrow bands since recent Hall effect measurements [11,12] indicate that a bandlike transport occurs in a single crystal of rubrene, a van der Waals-bonded organic semiconductor.

Heating the substrate at about 100 °C erases rings of C_{60} polymers. The activation energy for the thermal depolymerization has been determined to be 1.25 [10] and 1.75 eV for dimer [13]. The intermolecular bonding in C_{60} polymers is now understood in terms of the formation of a four-membered ring located between adjacent C_{60} molecules through [2 + 2] cycloaddition. The depolymerization can also be induced by injected carriers through the vibrational excitation of the bonds in the four-membered ring without heating the sample, analogously with vibrational heating induced by inelastic electron tunneling [6]. In this case the E_d value would be the same as the activation energy for the thermal depolymerization (1.25 or 1.75 eV).

A charge transfer (CT) excitonic mechanism and an ionic reaction mechanism were proposed as possible mechanisms for polymerization of C_{60} molecules in a STM configuration [14]. In the former mechanism, a triplet Frenkel exciton formed by injected carriers relaxes into a self-trapped triplet CT exciton state which is a precursor state for polymerization [15]. In this case the value of E_P must include not only the formation energy of the triplet Frenkel exciton (1.2 and 1.8 eV [16]) but also the activation energy for the subsequent dimerization from the precursor state (calculated as 2.5 eV [17]). Thus, $E_P < E_d$ cannot be satisfied, which is inconsistent with our proposed model for the ring formation.

In an ionic reaction mechanism, one of the two molecules to be polymerized accepts an electron or a hole. The [2 + 2] cycloaddition becomes a thermally allowed reaction prescribed by the Woodward-Hoffmann rules [18]. In this mechanism, depolymerization different from the vibrational excitation can be expected through a thermally allowed backreaction. Since the activation energy for the ionic polymerization must be lower than that for the ionic backreaction (depolymerization) as shown in Fig. 3(b), $E_P < E_d$ is strictly satisfied. Therefore, the ionic reaction mechanism is consistent with our proposed model. Furthermore, the fact that ionic polymerization in A_1C_{60}-type ($A = K$, Rb, Cs) compounds occurs spontaneously below a certain transition temperature [19] indicates the low E_P for the ionic polymerization. Consequently, it is suggested that the ring of C_{60} polymers is formed through ionic reaction induced by propagating carriers.

As is seen from Fig. 2, polymers are little observed in the interior of rings. In order for polymerization to take place, adjacent C_{60} molecules must adopt a specific configuration suitable for the [2 + 2] cycloaddition. It takes some time for C_{60} molecules to achieve this configuration because adjacent C_{60} molecules rotate independently at room temperature. An injected carrier must reside at a specific single C_{60} molecule at least for the configurationally required time. On the other hand, such time is not required for depolymerization. Therefore, the probability of polymerization would be lower than that of depolymerization; polymers tend to be little observed inside a ring.

It is worthy to mention the effect of duration of applied voltage pulses on the ring pattern. The pulse duration determines the number of injected carriers. Fifteen 30 s pulses with V_S of −3.0 V were necessary to obtain the ring shown in Fig. 2(a). At the different point in the close-packed layer, however, even one pulse was possible to produce a ring which had almost the same shape. The strong position dependence of the total injected carriers necessary for the ring formation may be explained by inhomogeneous distribution of a preexisting stress which is considered as a driving force of the polymerization [20]. In addition, it was found that the outer diameter of the resultant rings was not affected by the total number of injected carriers. On the other hand, a ring structure exhibiting polymers around the center of the ring [Fig. 2(c)] was produced by varying the total number through the successive injection. If the difference in reaction probabilities between polymerization and depolymerization defines a polymer pattern, the final distribution of polymers should no longer change its shape by further injection. Hence it is considered that the rings shown in Fig. 2 do not present a steady state. Actually, subsequent hole injection at the same energy into the ring shown in Fig. 2(c) produced a ring without polymers around its center (not shown), and further application of ten 30 s pulses did not repolymerize around the center. This result suggests that the steady-state distribution would be ring shaped after all. Therefore, varying the number of injected carriers step by step allows us to examine an evolution process of a ring structure of C_{60} polymers.

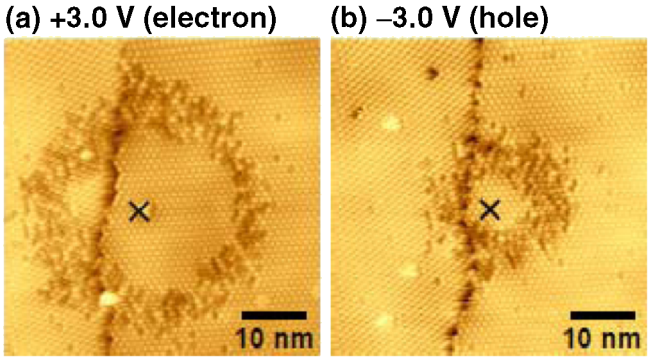

FIG. 4 (color online). Asymmetric rings of C_{60} polymers formed by carrier injection into close-packed layers with grain boundaries. STM images acquired after (a) electron injection at $V_S = +3.0$ V and (b) hole injection at -3.0 V into the marked points. The observed cracks refer to grain boundaries.

Another important feature of the series of STM images in Fig. 2 is the difference in the ring diameter between two rings formed by different carrier injections at the absolute bias value of 3.0 V [Figs. 2(a) and 2(d)]. This may be mainly attributable to the difference in the electron-phonon coupling constant λ. Since the degeneracies of HOMO and HOMO-1 are larger than those of LUMO and LUMO + 1, λ in hole-injected cases should be larger than that in electron cases [21]. Therefore, propagating holes may dissipate their energies faster than electrons, producing a smaller ring.

It appears that rings of C_{60} polymers can be regarded as a direct reflection of carrier propagation. To investigate this we have studied the effect of scatterers on carrier propagation by injecting carriers into close-packed layers with two types of defects. Figure 4 shows rings formed by carrier injection into the layers with three-dimensional (3D) defects. The cracks observed in the STM images indicate grain boundaries formed at the interface between two close-packed layers with different growth directions. The injection of electrons [Fig. 4(a)] and holes [Fig. 4(b)] into the marked points resulted in asymmetric rings. Carrier injection into the layer opposite to that with the marked points also produced an asymmetric ring, where the diameter of the ring is larger in the carrier-injected layer (not shown). This result rules out the possibility that the asymmetry is formed by the difference in structural and electronic characters between two close-packed layers. Therefore, we conclude that carrier scattering at grain boundaries produces such asymmetric rings. By contrast, carrier injection into a C_{60} close-packed layer with void defects only in the top layer exhibited no scattering effect (not shown). These results evidence 3D propagation of carriers in the C_{60} close-packed layer. The 3D propagation is also verified by the fact that polymerization was induced along both vertical and lateral directions [Fig. 1(c)].

In conclusion, a ring-shaped distribution of polymerized C_{60} molecules was produced by the radial propagation and energy dissipation of carriers injected from a STM tip. Both polymerization of C_{60} monomers and depolymerization are induced by injection of both electrons and holes, and carrier propagation can result in rings with various diameters conditioned by incident energy and type of carriers. The scattering of carriers by a grain boundary is clearly visualized and the carrier propagation is not influenced by the defects formed only in the top layer, showing 3D carrier propagation in the C_{60} close-packed multilayer. Consequently, this study has allowed us to elucidate the nanoscale propagation of carriers. Furthermore, the arrangements of scatterers upon the close-packed layer of C_{60} will provide a method for examining the physical picture of carrier scattering and for controlling the direction and spread of carrier propagation.

We are grateful to J. P. Glusker, S. Kashino, H. Tanaka, K. Tsukagoshi, and S. Okada for their valuable discussions. This work was in part supported by the Okayama University COE Project, and by a Grant-in-Aid (No. 18340104) from MEXT, Japan.

*Electronic address: nouchi@cc.okayama-u.ac.jp
†Electronic address: kubozono@cc.okayama-u.ac.jp

[1] T.-C. Shen *et al.*, Science **268**, 1590 (1995).
[2] B. C. Stipe, M. A. Rezaei, and W. Ho, Phys. Rev. Lett. **79**, 4397 (1997).
[3] T. Komeda *et al.*, Science **295**, 2055 (2002).
[4] S. Fujiki *et al.*, Chem. Phys. Lett. **420**, 82 (2006).
[5] Y. B. Zhao *et al.*, Appl. Phys. Lett. **64**, 577 (1994).
[6] Y. Kim, T. Komeda, and M. Kawai, Phys. Rev. Lett. **89**, 126104 (2002).
[7] Y. Nakamura *et al.*, Surf. Sci. **528**, 151 (2003).
[8] M. Nakaya, T. Nakayama, and M. Aono, Thin Solid Films **464–465**, 327 (2004).
[9] R. Tycko *et al.*, Phys. Rev. Lett. **67**, 1886 (1991).
[10] Y. Wang *et al.*, Chem. Phys. Lett. **217**, 413 (1994).
[11] V. Podzorov *et al.*, Phys. Rev. Lett. **95**, 226601 (2005).
[12] J. Takeya *et al.*, Jpn. J. Appl. Phys. **44**, L1393 (2005).
[13] P. Nagel *et al.*, Phys. Rev. B **60**, 16 920 (1999).
[14] Y. Nakamura *et al.*, Appl. Phys. Lett. **85**, 5242 (2004).
[15] M. Ichida *et al.*, Chem. Phys. Lett. **289**, 579 (1998).
[16] D. Dick *et al.*, Phys. Rev. Lett. **73**, 2760 (1994).
[17] M. Suzuki, T. Iida, and K. Nasu, Phys. Rev. B **61**, 2188 (2000).
[18] S. Pekker *et al.*, Solid State Commun. **90**, 349 (1994).
[19] P. W. Stephens *et al.*, Nature (London) **370**, 636 (1994).
[20] Y. Nakamura, Y. Mera, and K. Maeda, Appl. Phys. Lett. **77**, 2834 (2000).
[21] M. Saito, Phys. Rev. B **65**, 220508 (2002).